

# Various Unique Coordination Patterns of Hg and DFT Calculations To Determine the Formation of a 3-D Supramolecular Framework by Covalent and Noncovalent Interactions

Hong-Ping Zhou,<sup>\*,†</sup> Peng Wang,<sup>†</sup> Ling-Xia Zheng,<sup>†</sup> Wen-Qian Geng,<sup>†</sup> Jian-Hui Yin,<sup>†</sup> Xiao-Ping Gan,<sup>†</sup> Guo-Yi Xu,<sup>†</sup> Jie-Ying Wu,<sup>†</sup> Yu-Peng Tian,<sup>\*,†,‡,§</sup> Yu-He Kan,<sup>§</sup> Xu-Tang Tao,<sup>‡</sup> and Min-Hua Jiang<sup>‡</sup>

Department of Chemistry, Anhui University, 230039 Hefei, People's Republic of China, State Key Laboratory of Crystal Materials, Shandong University, 250100 Jinan, People's Republic of China, Department of Chemistry, Huaiyin Teachers College, 223300 Huaian, People's Republic of China, and State Key Laboratory Coordination Chemistry, Nanjing University, 210093 Nanjing, People's Republic of China

Received: November 26, 2008; Revised Manuscript Received: January 16, 2009

By combining a large  $\pi$ -conjugated bidentate ligand **L**: 3,6-dipyrazole-N-ethylcarbazole with  $\text{HgI}_2$ , an extraordinary supramolecular coordination polymer,  $[\text{Hg}_4\text{L}_2\text{I}_8]_\infty$ , has been prepared. The crystal structures of the ligand and its coordination polymer were determined by X-ray crystallography, which shows three varied coordination modes especially the rare asymmetric quadruply bridged trinuclear moieties in  $[\text{Hg}_4\text{L}_2\text{I}_8]_\infty$ . Density functional theory (DFT) calculations (ADF) performed on model dimers show the roles of covalent and noncovalent interactions in establishing the three-dimensional architecture.

## Introduction

Crystal engineering of self-assembly coordination polymers containing metal ions and organic ligands is of great current interest not only because of their varied structures but also due to their potential properties such as magnetism, nonlinear optics, electronics, catalysis, and molecular recognition.<sup>1–3</sup> In the context of inorganic/organic hybrid materials, some intramolecular and intermolecular weak interactions having considerable dispersive—repulsive character and merging into van der Waals interactions, such as  $\pi$ – $\pi$  interactions, C–H $\cdots$ X contacts, and X $\cdots$ X have been employed as a driving force of the crystal packing,<sup>4–6</sup> and the M $\cdots$ X<sup>7</sup> contacts are observed frequently in the solid state.

On the basis of its physical and electronic properties, mercuric iodide has recently been the focus of many studies because of its important utility in fields such as optical detector and superconducting materials.<sup>8</sup> To the best of knowledge, the mercury(II) ion, which was made softer by iodine in the Hg–I system, has a versatile coordination number and can serve to link ligands to form polymeric compounds with novel coordination patterns. The most common coordination framework is four-coordination with  $\text{sp}^3$  hybridization in a tetrahedral geometry.<sup>9</sup> Sometimes the mercury(II) ion also adopts a six-coordination mode where Hg(II) situates in the inversion center with a distorted octahedral geometry,<sup>10</sup> while in a few compounds, the rare five-coordinated Hg(II) has been reported with a tetragonal pyramidal or trigonal bipyramidal geometry.<sup>11</sup> On the other hand, taking into account the large polarization of the mercury(II) ion, it shows a specific affinity to the rigid N-donor ligands. Carbazole-containing compounds, as is well-known, have been widely studied for the application of an electroluminescent (EL) device and fabrication of light-emitting diodes (LED).<sup>12</sup> As pyrazole is an electron-rich aromatic compound,

we introduced pyrazole groups to the carbazole ring in high yield, by Ullmann reaction according to the method of our previous paper.<sup>13</sup> The functionality for use in supramolecular architectures of the organic molecule (addition of donor atom N) allows its incorporation into the inorganic coordination complex, which has the advantage of higher thermal stability and solvent resistance than organic material.

Herein, we present the three-dimensional (3-D) structure of a novel self-assembly complex with  $\text{HgI}_2$  and the ligand (**L** = 3,6-bipyrazole-9-ethylcarbazole), where there exists three diversified coordination modes, especially the rare quadruply bridged trinuclear moieties. DFT calculations show that covalent and noncovalent interactions play crucial roles in establishing the three-dimensional architecture.

## Experimental Section

All chemicals and solvents were dried and purified by using common methods. Elemental analyses were performed with a Perkin-Elmer 240B element analyzer. IR spectra were recorded with a Nicolet FTIR 170SX instrument, using KBr pellets.

**Synthesis and Characterization.** 3,6-Dipyrazole-N-ethylcarbazole (**L**): **L** was synthesized by a two-step reaction according to the method of our previous paper.<sup>13</sup> Pale yellow needle single crystals suited for X-ray diffraction were obtained by slow evaporation of ethyl acetate at room temperature.

$[\text{Hg}_4\text{L}_2\text{I}_8]_\infty$ : **L** (40.00 mg, 0.10 mmol) and  $\text{HgI}_2$  (31.60 mg, 0.10 mmol) were dissolved in 20 mL of ethyl acetate. The mixture was refluxed for 2 h at 70 °C and then cooled to room temperature to give a clear solution. Pale yellow cuboid single crystals suitable for X-ray diffraction were obtained after several days by slow evaporation of the filtrate at room temperature. Yield: 91%. IR (KBr,  $\text{cm}^{-1}$ ): 2974 (w), 2928 (w), 1623 (m), 1516 (s), 1483 (s), 1401 (m), 1317 (m), 1225(m), 1191 (w), 1153 (w), 1118 (w), 1055 (m), 1033 (w), 946 (w), 871 (w), 797 (w), 748 (s), 669 (m). Anal. Calcd for  $\text{C}_{40}\text{H}_{34}\text{Hg}_4\text{I}_8\text{N}_{10}$ : C 19.43, H 1.39, N 5.67. Found C 19.16, H 1.40, N 5.91.

**X-ray Crystallography.** Single-crystal X-ray diffraction measurements were carried out on a Bruker Smart 1000 CCD

\* Corresponding author. E-mail: zhpzhp@263.net.

<sup>†</sup> Anhui University.

<sup>‡</sup> Shandong University.

<sup>§</sup> Huaiyin Teachers College.

<sup>#</sup> Nanjing University.

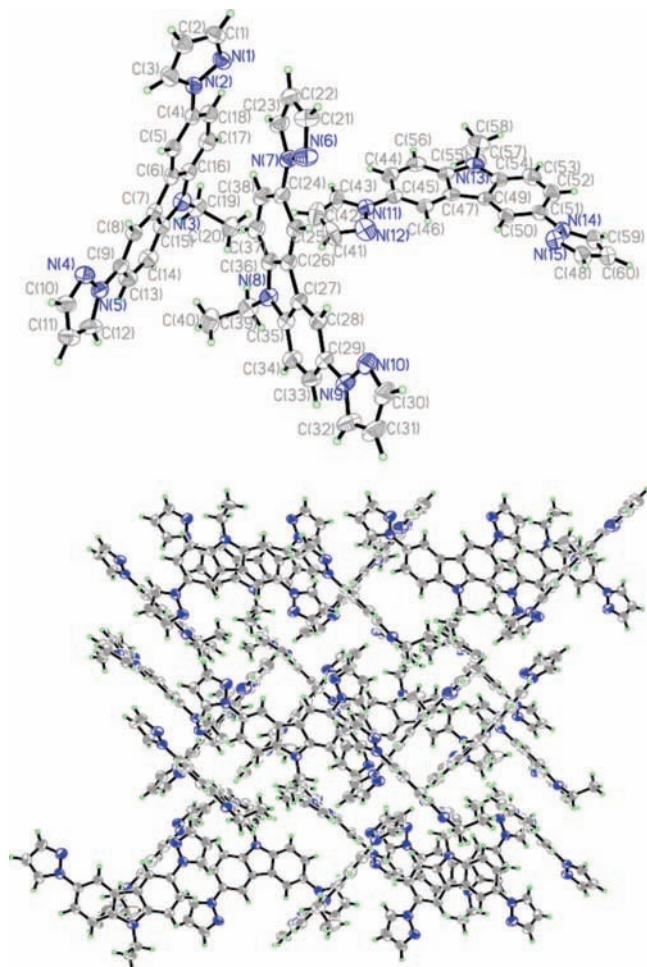


**Figure 1.** (a) ORTEP diagram showing the structure of compound L with thermal ellipsoids at the 30% probability level and the atom-labeling scheme and (b) molecular packing of compound L.

diffractometer equipped with a graphite crystal monochromator situated in the incident beam for data collection at room temperature. The determination of unit cell parameters and data collections were performed with Mo K $\alpha$  radiation ( $\lambda = 0.71073$  Å). Unit cell dimensions were obtained with least-squares refinements, and all structures were solved by direct methods with SHELXL-97.<sup>14</sup> The other non-hydrogen atoms were located in successive difference Fourier syntheses. The final refinement was performed by full-matrix least-squares methods with anisotropic thermal parameters for non-hydrogen atoms on  $F^2$ . The hydrogen atoms were added theoretically and riding on the concerned atoms. Crystallographic crystal data and processing parameters for L and  $[\text{Hg}_4\text{L}_2\text{I}_8]_\infty$  are shown in Table 1. Selected bond lengths and bond angles for  $[\text{Hg}_4\text{L}_2\text{I}_8]_\infty$  are listed in Table 2.

CCDC-675024 (for L) and CCDC-675027 (for the coordination polymer) contain the supplementary crystallographic data for this paper. These data can be obtained free of charge from The Cambridge Crystallographic Data Centre via [http://www.ccdc.cam.ac.uk/data\\_request/cif](http://www.ccdc.cam.ac.uk/data_request/cif).

**Computational Details.** DFT calculations<sup>15</sup> were carried out with the Amsterdam Density Functional (ADF-2006) program. The local spin density (LSD) exchange correlation potential was used with the local density approximation of the correlation energy (Vosko, Wilk, and Nusair).<sup>16</sup> Gradient-corrected geometry optimizations<sup>17</sup> were performed by using the generalized gradient approximation (Perdew–Wang nonlocal exchange and

**TABLE 1: Crystallographic Data for L and  $[\text{Hg}_4\text{L}_2\text{I}_8]_\infty$**

	L	$[\text{Hg}_4\text{L}_2\text{I}_8]_\infty$
formula	$\text{C}_{20}\text{H}_{17}\text{N}_5$	$\text{C}_{40}\text{H}_{34}\text{Hg}_4\text{I}_8\text{N}_{10}$
fw	327.39	2472.33
crystal system	triclinic	triclinic
space group	$P\bar{1}$	$P\bar{1}$
$a$ (Å)	12.750(3)	8.9615(19)
$b$ (Å)	13.084(3)	12.664(3)
$c$ (Å)	17.528(4)	24.099(5)
$\alpha$ (deg)	98.19(3)	100.117(3)
$\beta$ (deg)	107.60(3)	95.283(3)
$\gamma$ (deg)	110.76(3)	92.318(3)
$V$ (Å <sup>3</sup> )	2502.0(9)	2676.5(10)
$Z$	6	2
$d_{\text{calcd}}$ (g/cm <sup>3</sup> )	1.304	3.068
$\mu$ (cm <sup>-1</sup> )	0.081	16.089
$F(000)$	1032	2176
crystal size	$0.2 \times 0.1 \times 0.1$	$0.10 \times 0.20 \times 0.09$
no. of data/restraint/parameters	9984/0/676	10271/0/559
no. of reflns collected	11775	14105
no. of unique reflns	9984	9399
goodness of fit	0.899	0.939
$R_1$ [ $I > 2\sigma(I)$ ]	0.0522	0.0670
$wR_2$ [ $I > 2\sigma(I)$ ]	0.1224	0.1664
$R_1$ (all data)	0.1196	0.1345
$wR_2$ (all data)	0.1459	0.1957
residuals (e $\cdot$ Å <sup>-3</sup> )	0.204, -0.277	2.185, -2.223

correlation corrections-PW91).<sup>18</sup> A triple- $\zeta$  Slater type orbital (STO) basis set augmented by two polarization functions was used for Hg, N, I, C, and H. A frozen core approximation was used to treat the core electrons: (1s) for C and N; (4p) for I; and (4d) for Hg. Relativistic effects were accounted for with the ZORA approximation.<sup>19</sup> The selected fragments (Figures 5 and 6) were cut out directly from the CIF data without optimization. Fragments analysis is performed on two relative fragments for investigation on the attractive energy between them. And further calculations are carried out to include the strong coordinate interaction. Normal energies also were calculated based on the model optimized from the CIF data to obtain the energy between the two fragments except for the interaction from  $\pi \rightarrow \pi$ , which could not be optimized but could be obtained from the typical experiment report.<sup>20</sup>

## Results and Discussion

**Structure of L.** The ligand crystallizes in the triclinic space group  $P\bar{1}$ , with 3 molecules per unit cell. The whole skeleton structure, including two pyrazole rings and a carbazole unit, possesses good planarity. The dihedral angles between the two pyrazole rings and the central carbazole unit range from  $1.70^\circ$  to  $13.28^\circ$ . The adjacent molecules are stacked through strong  $\pi-\pi$  interactions with the shortest intermolecular distance of 3.376 Å. Figure 1 shows the structures of compound L and its packing diagram.

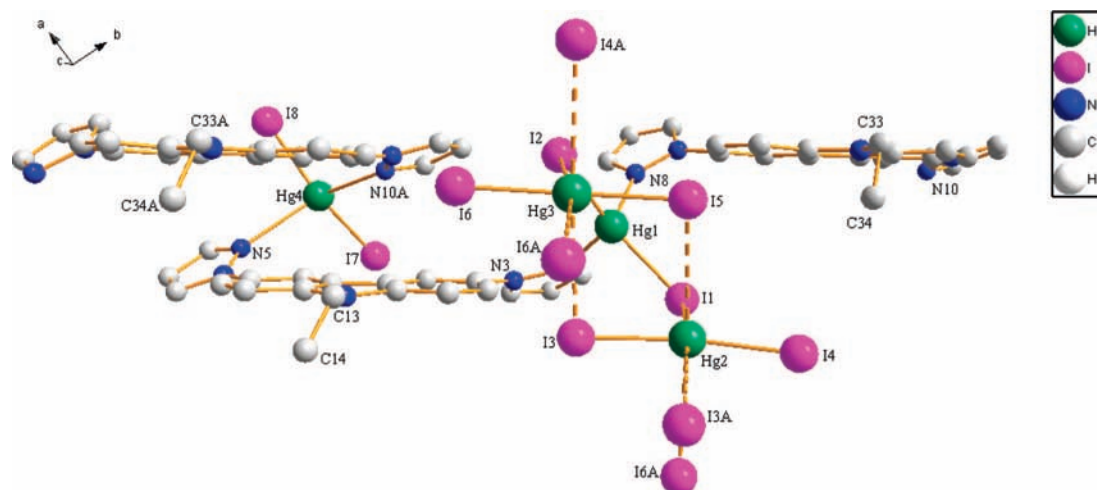
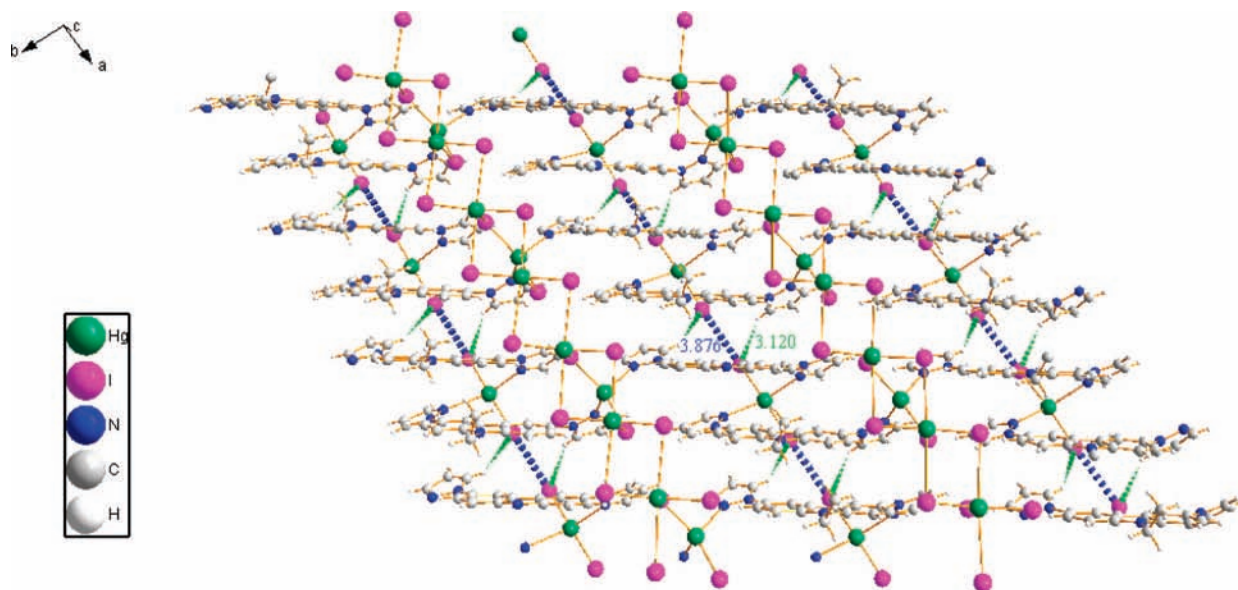
**Structure of  $[\text{Hg}_4\text{L}_2\text{I}_8]_\infty$ .** The metal coordination polymer  $[\text{Hg}_4\text{L}_2\text{I}_8]_\infty$  crystallizes in the triclinic space group  $P\bar{1}$  as shown in Figure 2, which at first sight reveals an extremely large distortion with the dihedral angle between the two pyrazole rings and the central carbazole unit ranging from  $19.12^\circ$  to  $38.38^\circ$ . The great deviation is probably due to the strong preference of metal for soft donors with large atom size such as the iodine atoms and a weak preference for N atoms.<sup>21</sup>

As shown in Figure 2, the ligand 3,6-bipyrazole-9-ethylcarbazole,  $\text{Hg}^{2+}$  cations, and  $\text{I}^-$  anions are interconnected with three diversified coordination patterns of some interesting structural characteristics. Hg(1) adopts a much distorted tetrahedral geometry with two pyrazole-N atoms from two individual ligands with bond lengths of 2.397(15) and 2.433(19) Å and

**TABLE 2: Selected Bond Lengths (Å) and Angles (deg) for [Hg<sub>4</sub>L<sub>2</sub>I<sub>8</sub>]<sub>∞</sub><sup>a</sup>**

Hg1–N3	2.433(19)	Hg1–N8	2.397(15)	Hg1–I1	2.653(18)
Hg1–I2	2.646(18)	Hg2–I1	3.228(2)	Hg2–I3	2.621(16)
Hg2–I4 <sup>b</sup>	2.614(18)	Hg3–I2	3.285(2)	Hg3–I5	2.613(18)
Hg3–I6 <sup>c</sup>	2.623(16)	Hg4–N5 <sup>d</sup>	2.684(18)	Hg4–N10A <sup>e</sup>	2.795(18)
Hg4–I7 <sup>d</sup>	2.608(18)	Hg4–I8 <sup>d</sup>	2.602(18)	N3–Hg1–N8	88.0(6)
N8–Hg1–I2	97.3(5)	N3–Hg1–I2	114.6(4)	I1–Hg1–I2	141.80(7)
Hg1–I1–Hg2	103.32(6)	Hg1–I2–Hg3	103.47(5)	I4 <sup>b</sup> –Hg2–I3	167.45(7)
I2–Hg3–I6 <sup>c</sup>	88.26(5)	I7 <sup>d</sup> –Hg4–I8	155.36(7)	N5 <sup>d</sup> –Hg4–N10A <sup>e</sup>	116.46(6)

<sup>a</sup> Symmetry code. <sup>b</sup> 1 + x, y, z. <sup>c</sup> -1 + x, y, z. <sup>d</sup> -1 + x, -1 + y, z. <sup>e</sup> 1 + x, 1 + y, z.

**Figure 2.** Coordination environments of Hg with the atom numbering scheme; H atoms were omitted for clarity.**Figure 3.** The 2-D framework of complex [Hg<sub>4</sub>L<sub>2</sub>I<sub>8</sub>]<sub>∞</sub> showing the weak C–H⋯I (green) interactions and I⋯I (blue) interactions along the *a*-axis.

two asymmetric bridging I atoms with bonds of 2.653(18) and 2.646(18) Å (Table 2). The bond angles I1–Hg1–I2, N3–Hg1–N8, I2–Hg1–N3, and N8–Hg1–I2 are 141.80(7)°, 88.0(6)°, 114.6(4)°, and 97.3(5)°, respectively, while Hg(4) also locates in a four-coordination environment chelating with two terminal I atoms with bonds of 2.602(18) and 2.608(18) Å and two N donors with bonds of 2.684(18) and 2.795(18) Å. However, of particular interest here are the coordination environments of Hg(2) and Hg(3), both with six bridging I atoms around them. As we know, the sum of covalent radii for I and Hg in the linear coordination is 2.63 Å.<sup>22</sup> Taking the two short bond length of Hg3–I5 and Hg3–I6 to be 2.613 and 2.623 Å

with the angle of I5–Hg3–I6 to be 171.41°, we can safely define the two as covalent interactions, while the other four bond lengths Hg3–I2, Hg3–I3, Hg3–I4A, and Hg3–I6A of 3.285, 3.477, 3.575, and 3.603 Å, respectively (shown in Table 2) are noncovalent interactions. Consequently, we propose the coordination of mercury by iodine is octahedral 2 + 4, with two close and four considerably more distant neighbors. Surprisingly, the packing of the iodine atoms is perfectly octahedral geometry without distortion. Obviously, as a member of the d<sup>10</sup> configuration of the IIB metal ions, Hg(II) has a high coordination number and behaves as a soft Lewis base, making it much easier to coordinate with I atom and thus form the [Hg<sub>2</sub>I<sub>2</sub>]<sup>2+</sup> ring. The

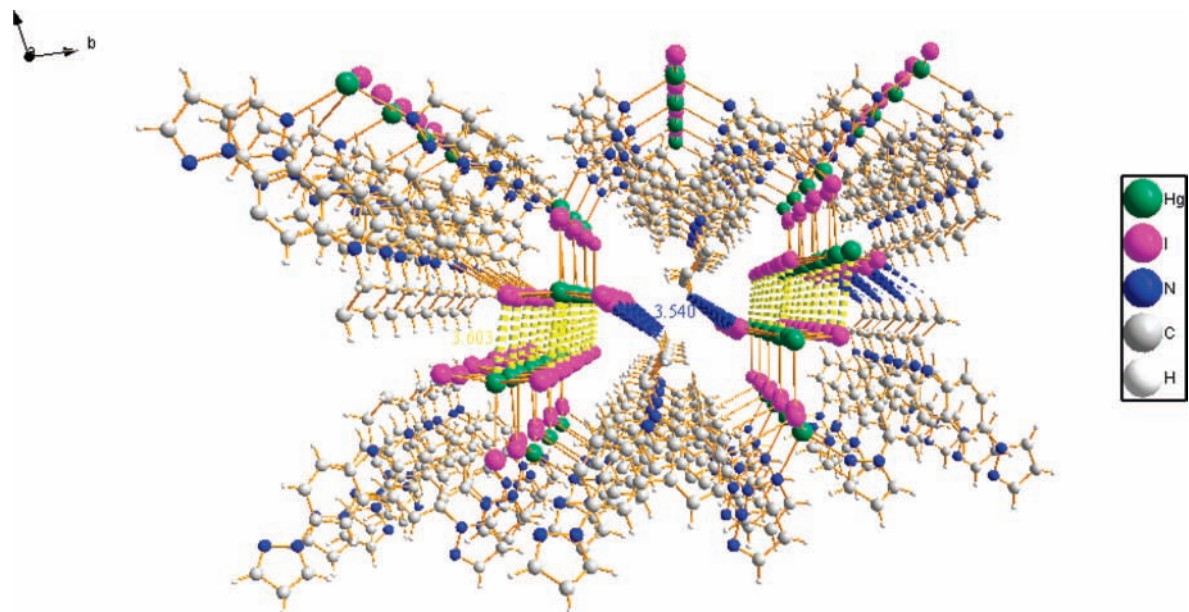


**Figure 4.** The 3-D architecture is connected by the weak C–H...I (blue) interactions between ethyl C–H and bridging I and Hg...I (yellow) interactions.

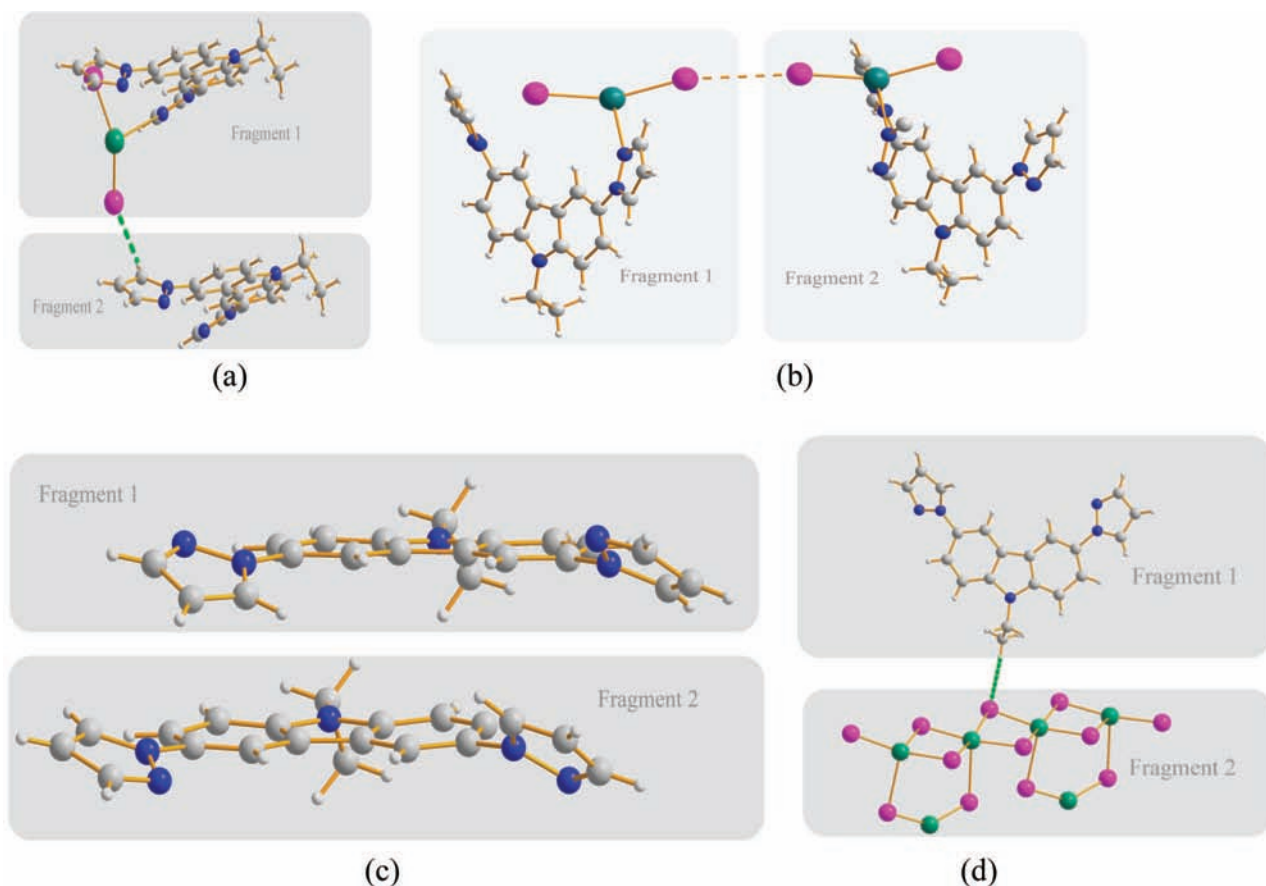


**Figure 5.** (a) Fragments selected for C–H...I (2-D) interactions; (b) fragments selected for I...I interactions; (c) fragments selected for  $\pi$ – $\pi$  interactions; and (d) fragments selected for only one C–H...I (3-D) interaction.

internuclear distances of Hg...Hg within the Hg–( $\mu$ I)<sub>2</sub>–Hg moieties are 4.483 Å, which are much longer than the sum of van der Waals radii (1.7 Å)<sup>23</sup> of the two mercury atoms, indicating the absence of significant bonding interactions between the Hg atoms in the molecular structures.

Seen along the crystallographic *ab*-plane, an infinite zigzag 1-D chain is formed by self-assembly of [Hg<sub>4</sub>L<sub>2</sub>I<sub>8</sub>] moieties by

**TABLE 3: Energy of Weak Interactions in Establishing 2-D and 3-D Frameworks**

	weak interaction	energy (kJ/mol)	further calcn	normal energy
Figure 5a	C–H...I (2-D)	–3.16	–2.88	–10.10
Figure 5b	I...I	–1.46	–2.21	–2.47
Figure 5c	$\pi$ – $\pi$	–2.03	–2.33	–2.4 ± 0.4
Figure 5d	C–H...I (3-D)	–7.32	–7.81	–7.58

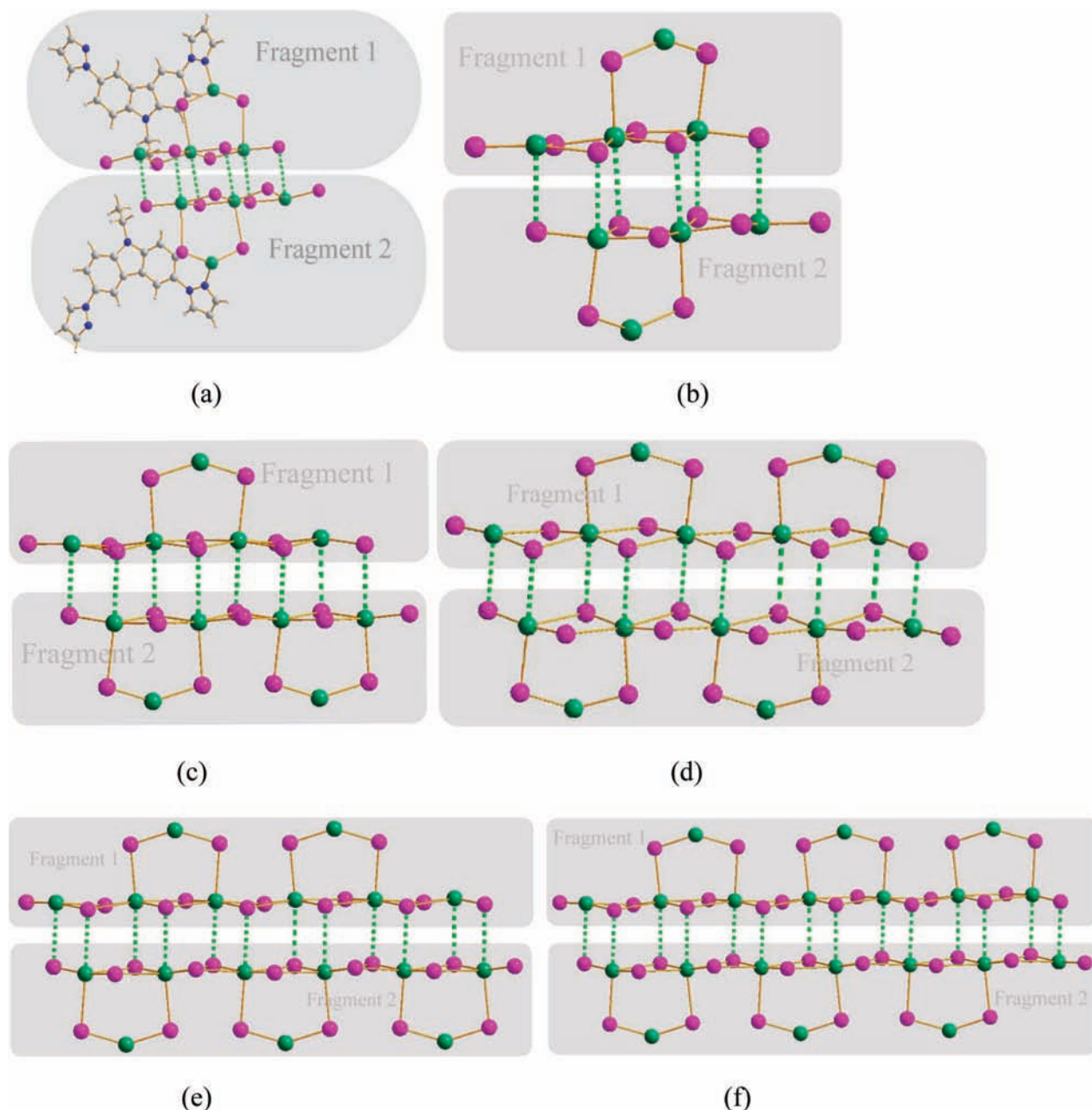


**Figure 6.** (a) Fragments selected for six Hg $\cdots$ I interactions and two ligands; (b) fragments selected for six Hg $\cdots$ I interactions; (c) fragments selected for eight Hg $\cdots$ I interactions; (d) fragments selected for ten Hg $\cdots$ I interactions; (d) fragments selected for twelve Hg $\cdots$ I interactions; and (e) fragments selected for fourteen Hg $\cdots$ I interactions.

coordination of the metal-bound peripheral pyrazole-N of this unit to the neighboring Hg center running “parallel” to one another (Hg $\cdots$ Hg distances of 9.309 and 9.230 Å, and an Hg4A $\cdots$ Hg1 $\cdots$ Hg4 angle of 117.01°). While seen along the *a*-axis, another extraordinary 1-D chain is formed by a dimeric halogen-bridged molecule (M–I–M), via two I atoms bridged between two different mercury atoms to build doubly Hg2–( $\mu$ I)<sub>2</sub>–Hg3 with two different Hg–I (bridging) distances of 2.613 and 3.493 Å and the Hg<sub>2</sub>I<sub>2</sub> rectangle motifs with I3–Hg2–I5 angles of 85.98° and Hg2–I3–Hg3 angles of 93.58°, respectively (Figure 2). To our knowledge, the formation of the four-membered [Hg<sub>2</sub>I<sub>2</sub>]<sup>2+</sup> ring is common in mercury complexes.<sup>24</sup> However, the extremely asymmetric quadruply bridged trinuclear moieties, just like “pillars” upholding the zigzag chains, are rather rare. Here, the seven-membered [Hg<sub>3</sub>I<sub>4</sub>] basket-like motifs and the terminal I bridge are setting up on the zigzag chains alternated with each other to generate a 2-D

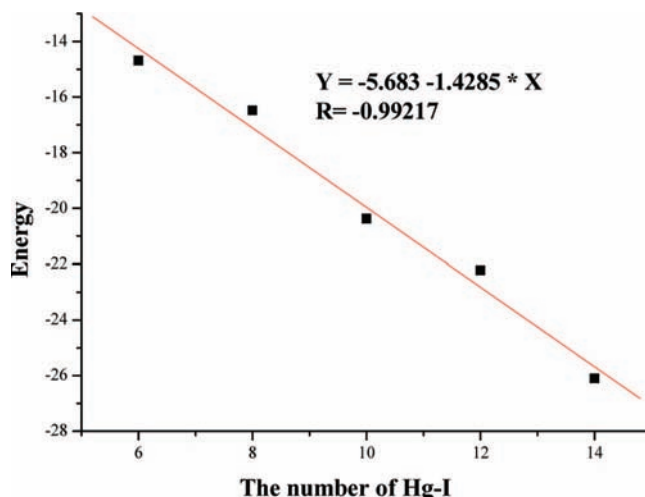
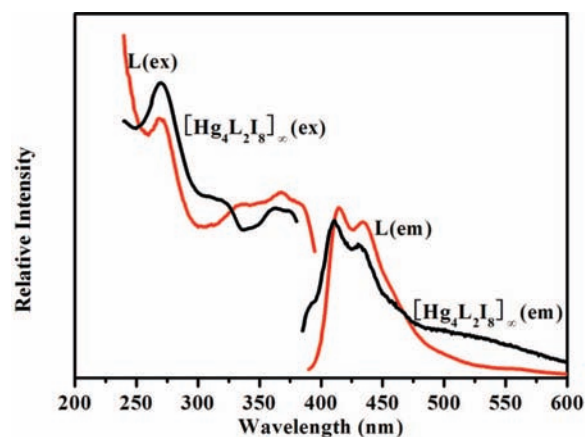
supramolecular network, which makes a crucial contribution to the stability of the metal complex. Directional interactions formed between the halogen are specific attractive induced force and have been used intensively in systematic crystal engineering.<sup>25</sup> Mindful of the compact and ordered arrangement, many weak interactions are induced:  $\pi$ – $\pi$  stacking and I $\cdots$ I and C–H $\cdots$ I weak interactions. The shortest distance of  $\pi$ – $\pi$  intermolecular interactions between adjacent zigzag chains is 3.376 Å. As reported previously, an I–I distance of less than 3.96 Å is considered to have I $\cdots$ I interactions<sup>26</sup> and the range of H $\cdots$ I of about 3.35 Å,<sup>13</sup> while the distance here between two terminal I atoms from two adjacent zigzag chains is 3.876 Å, and the extensive hydrogen-bond network of the shortest I $\cdots$ H is 3.120 Å (C–H $\cdots$ I is 3.958 Å and the angle is 150.83°) between pyrazole C–H and terminal I (Figure 3). Thus they obviously appear to be significant factors which can make an additional contribution to the stability of this complex.

**TABLE 4: Energy of Weak Interactions in Different Numbers of Hg⋯I Models**

	model selected	energy (kJ/mol)
Figure 6a	six Hg⋯I and two L	-18.16
Figure 6b	six Hg⋯I	-14.68
Figure 6c	eight Hg⋯I	-16.48
Figure 6d	ten Hg⋯I	-20.37
Figure 6e	twelve Hg⋯I	-22.21
Figure 6f	fourteen Hg⋯I	-26.10

Additionally, taking the van der Waals radii of Hg and I to be 1.70 and 2.15 Å,<sup>23</sup> respectively, any Hg⋯I contact less than 3.85 Å may therefore potentially be considered significant, while the shortest distance between Hg and I in this complex is 3.603 Å, which can be defined as a weak contact giving the octahedral 2 + 4 effective coordination of mercury. Interestingly, as mentioned above, the range of H⋯I is about 3.35 Å,<sup>13</sup> while according to the theoretical calculations (see DFT Calculations), this structure seems to consist of an unusual extensive weak interaction between ethyl C–H and bridging I, the shortest I⋯H is 3.540 Å, C–H⋯I is 4.331 Å, and the angle is 141.23° (Figure 4), and consequently further extends into a 3-D supramolecular architecture. Theoretical calculations (see DFT Calculations) show that both contacts account for significance in the stability of this metal complex.

**DFT Calculations.** DFT calculations (ADF) program were carried out to determine the energies associated with the formation of 3-D architecture in this supramolecule  $[\text{Hg}_4\text{L}_2\text{I}_8]_\infty$  and to better understand the weak interactions as will be discussed below. The orbital analysis shows us that I (4p) plays a very important role in the stabilized structure, not only in Hg⋯I strong coordination bonds (-18.16 kJ/mol), but also in I⋯I weak interactions as small as -1.46 kJ/mol. Seen from Table 3 and Figure 5, in the 2-D framework, the correlated energies for C–H⋯I, I⋯I, and  $\pi$ - $\pi$  are approximately -3.16, -1.46, and -2.03 kJ/mol, respectively. In the 3-D architectures, the correlated energy of six Hg⋯I is -18.16 kJ/mol while the interacted energy for only one C–H⋯I is -7.32 kJ/mol. The normal energies are obtained after optimization. Compared with the normal energies, all the above energies for weak interactions are more or less weaker, indicating that there are no deformations caused by the unique coordination patterns. It is well-known the molecular interactions are not only dependent on the molecular geometries but also on the electronic distributions in the molecules. So further investigation including the electronic distributions on the model takes into account the strong Hg⋯N bonds in the new models. To exclude the other weak interaction that may influence the interaction we are interested in, certain  $\text{HgI}_2$  units in each model are carefully selected to avoid the undesired interactions, see the information deposited with the CCDC. All the models are calculated by adding a new  $\text{HgI}_2$  unit, except the interaction from the Hg⋯I bond. The simulated result indicates that the further calculation deviates from the former calculation by about 10%, meaning that the former model selected could stand for the certain interaction we focused on. The simulated Hg⋯I energy is very sensitive to the model selected due to strong interaction from the Hg⋯I bonds. To obtain the energy to reflect the true interaction between the two fragments, five models that include  $\text{HgI}_2$  units only are selected (Figure 6b–f). The linear relationship between the number of Hg⋯I bonds and the interaction energy are obtained with a deviation factor  $R = -0.99217$ , indicating that they fit the linear very well (Figure 7 and Table 4) and showing that the model selected could reflect the interaction from the two fragments. To further obtain the L influence on the interaction, two ligands

**Figure 7.** Linear relationship between the number of Hg–I and correlated energy.**Figure 8.** Solid-state emission spectra of L and its metal complex at room temperature: red, L; black,  $[\text{Hg}_4\text{L}_2\text{I}_8]_\infty$ .

are selected in the six Hg⋯I model (Figure 6a). The outcomes show that each L will lower the energy by 1.74 kJ/mol, which is far from the former theoretical study by no more than 10%. In some sense, the weak interactions could be evaluated by this simple method.

**Luminescent Properties.** Luminescent transition-metal complexes containing multichromophoric ligands with extended conjugation have been extensively studied in recent years, partly because of their potential use as sensors, probes,<sup>27</sup> and photonic devices.<sup>28</sup> Owing to the ability to affect the emission wavelength of organic materials, syntheses of inorganic–organic coordination complexes by the judicious choice of organic spacers and transition-metal centers can be an efficient method for obtaining new types of electroluminescent materials.<sup>29</sup> Free ligand and its metal complex show emission in the solid state at room temperature, exhibiting different properties (see Figure 8). Free L presents an emission maximum at 414 nm with a shoulder peak at about 435 nm, which is completely invariant upon excitation in the range of 270–369 nm, while the metal complex exhibits similarly strong emission intensity as the L, which can be tentatively assigned to the ligand-to-ligand charge transfer (LLCT). Obviously, as shown in Figure 8, the  $[\text{Hg}_4\text{L}_2\text{I}_8]_\infty$  has shown a blue shift of several nanometers, probably due to the worse planarity of  $[\text{Hg}_4\text{L}_2\text{I}_8]_\infty$  increasing the energy of the whole system, in consideration of the huge steric hindrance caused by the unique coordination patterns.

## Conclusion

In summary, the novel metal complex with three unique coordination patterns has been synthesized and analyzed. Mainly, we discussed the weak interactions such as  $I\cdots I$ ,  $Hg\cdots I$ , and  $C-H\cdots I$  caused by the extraordinary coordination patterns especially the rare asymmetric quadruply bridged trinuclear moieties in  $[Hg_4L_2I_8]_{\infty}$ . DFT calculations performed on model dimers lead to interaction energies in the 2-D and 3-D frameworks and support the knowledge that  $Hg-I$  covalent and other noncovalent interactions give rise to the strongest interaction in establishing 3-D supramolecular architecture, which definitely shows that intramolecular and intermolecular weak interactions act as a driving force in the crystal engineering. On the other hand, the experimental results indicate that the luminescence maximum of the coordination polymer was apparently blue-shifted compared to that of the free ligand probably attributed to the steric hindrance caused by the unique coordination patterns.

**Acknowledgment.** The work was supported by grants from the National Natural Science Foundation of China (50532030, 50703001, 20771001), the Natural Science Foundation of Anhui Province (070414188), Education Committee of Anhui Province (2006KJ032A), the Team for scientific Innovation Foundation of Anhui Province (2006KJ007TD), the Young Teacher Foundation of Institution of High Education of An Hui Province (2007jq1019), the Ministry of Education and Person with Ability Foundation of Anhui University, and the Key Laboratory of Functional Inorganic Materials Chemistry of Anhui Province.

## References and Notes

- (1) (a) Kitagawa, S.; Kitaura, R.; Noro, S. *Angew. Chem., Int. Ed.* **2004**, *43*, 2334. (b) Liu, C.-S.; Shi, X.-S.; Li, J.-R.; Wang, J.-J.; Bu, X.-H. *Cryst. Growth Des.* **2006**, *6*, 656. (c) Eddaoudi, M.; Moler, D. B.; Li, H.; Chen, B.; Reineke, T. M.; O'Keeffe, M.; Yaghi, O. M. *Acc. Chem. Res.* **2001**, *34*, 319. (d) Telfer, S. G.; Kuroda, R. *Coord. Chem. Rev.* **2003**, *242*, 33. (e) Barnett, S. A.; Champness, N. R. *Coord. Chem. Rev.* **2003**, *246*, 145. (f) Berryman, O. B.; Bryantsev, V. S.; Stay, D. P.; Johnson, D. W.; Hay, B. P. *J. Am. Chem. Soc.* **2007**, *129*, 48.
- (2) (a) Vittal, J. J. *Coord. Chem. Rev.* **2007**, *251*, 1781. (b) Wu, C.-D.; Hu, A.; Zhang, L.; Lin, W. *J. Am. Chem. Soc.* **2005**, *127*, 8940. (c) Moulton, B.; Zaworotko, M. *J. Chem. Rev.* **2001**, *101*, 1629. (d) Tabares, L. C.; Navarro, J. A. R.; Salas, J. M. *J. Am. Chem. Soc.* **2001**, *123*, 383. (e) Lin, K. *J. Angew. Chem., Int. Ed.* **1999**, *38*, 2730. (f) Sun, Y.; Gates, B.; Mayers, B.; Xia, Y. *Nano Lett.* **2002**, *2*, 165.
- (3) (a) Biradha, K.; Sarkar, M.; Rajput, L. *Chem. Commun.* **2006**, 4169. (b) Robson, R.; Abrahams, B. F.; Batten, S. R.; Gable, R. W.; Hoskins, B. F.; Liu, J. *Supramolecular Architecture*; American Chemical Society: Washington, DC, 1992; Chapter 19. (c) Braga, D.; Grepioni, F.; Orpen, A. G., Eds. *Crystal Engineering: From Molecules and Crystals to Materials*; Kluwer: Dordrecht, The Netherlands, 1999; NATO Science Series, Series C, Vol. 538. (d) Biradha, K.; Seward, C.; Zaworotko, M. *J. Angew. Chem., Int. Ed.* **1999**, *38*, 492. (e) Munakata, M.; Wu, L. P.; Kuroda-Sowa, T. *Bull. Chem. Soc. Jpn.* **1997**, *70*, 1727.
- (4) (a) Mahmoudi, G.; Morsali, Ali. *Cryst. Growth Des.* **2008**, *8*, 391. (b) Aakeröy, C. B.; Beatty, A. M.; Leinen, D. S. *Angew. Chem., Int. Ed.* **1999**, *38*, 1815. (c) Desiraju, G. R. *Angew. Chem., Int. Ed. Engl.* **1995**, *34*, 2311. (d) Burrows, A. D.; Harrington, R. W.; Mahon, M. F.; Price, C. E. *J. Chem. Soc., Dalton Trans.* **2000**, 3845. (e) Lehn, J. M. *Supramolecular Chemistry*; VCH: Weinheim, Germany, 1995. (f) Raj, M. M.; Dharmaraja, A.; Kavitha, S. J.; Panchanatheswaran, K.; Lynch, D. E. *Inorg. Chim. Acta* **2007**, *360*, 1799.
- (5) (a) Li, X. P.; Zhang, J. Y.; Liu, Y.; Pan, M.; Zheng, S. R.; Kang, B. S.; Su, C. Y. *Inorg. Chim. Acta* **2007**, *360*, 2990. (b) Kong, L. Y.; Zhu, H. F.; Okamura, T.; Sun, W. Y.; Ueyama, N. *J. Solid State Chem.* **2004**, *177*, 2271. (c) Liu, H. J.; Tao, X. T.; Yang, J. X.; Yan, Y. X.; Ren, Y.; Zhao, H. P.; Xin, Q.; Yu, W. T.; Jiang, M. H. *Cryst. Growth Des.* **2008**, *8*, 259. (d) Taylor, R.; Kennard, O. *Acc. Chem. Res.* **1984**, *17*, 320. (e) Steiner, T. *Angew. Chem., Int. Ed.* **2002**, *41*, 48.
- (6) (a) Wang, X. F.; Lv, Y.; Okamura, T.; Kawaguchi, H.; Wu, G.; Sun, W. Y.; Ueyama, N. *Cryst. Growth Des.* **2007**, *7*, 1125. (b) Dziubek, K. F.; Katrusiak, A. *J. Phys. Chem. B* **2008**, *112*, 12001. (c) Desiraju, G. R.

- Acc. Chem. Res.* **2002**, *35*, 565. (d) Ghosh, M.; Biswas, P.; Flörke, U.; Nag, K. *Inorg. Chem.* **2008**, *47*, 281. (e) Ciunik, Z.; Desiraju, G. R. *Chem. Commun.* **2001**, 703. (f) Raj, M. M.; Dharmaraja, A.; Kavitha, S. J.; Panchanatheswaran, K.; Lynch, D. E. *Inorg. Chim. Acta* **2007**, *360*, 1799.
- (7) (a) Zhilyaeva, E. I.; Kovalevsky, A. Y.; Lyubovskii, R. B.; Torunova, S. A.; Mousdis, G. A.; Papavassiliou, G. C.; Lyubovskaya, R. N. *Cryst. Growth Des.* **2007**, *7*, 2768. (b) Zeng, Q. D.; Li, M.; Wu, D. X.; Lei, S. B.; Liu, C. M.; Piao, L. Y.; Yang, Y. L.; An, S. Y.; Wang, C. *Cryst. Growth Des.* **2008**, *8*, 869.
- (8) (a) Yoon, J. B.; Jang, E. S.; Kwon, S. J.; Ayrall, A.; Cot, L.; Choy, J. H. *Bull. Korean Chem. Soc.* **2001**, *22*, 1111. (b) Wang, J.; Qian, X. *Chem. Commun.* **2006**, 109. (c) Zheng, H.; Qian, Z. H.; Xu, L.; Yuan, F. F.; Lan, L. D.; Xu, J. G. *Org. Lett.* **2006**, *8*, 859.
- (9) (a) Sabounchei, S. J.; Nemattalab, H.; Salehzadeh, S.; Bayat, M.; Khavasi, H. R.; Adams, H. J. *Organomet. Chem.* **2008**, *693*, 1975. (b) Li, L. K.; Song, Y. L.; Hou, H. W.; Liu, Z. S.; Fan, Y. T.; Zhu, Y. *Inorg. Chim. Acta* **2005**, *358*, 3259. (c) Ebrahim, M. M.; Stoekli-Evans, H.; Panchanatheswaran, K. *Polyhedron* **2007**, *26*, 3491. (d) Louise, J. M.; William, H.; Brian, K. N. *Polyhedron* **1998**, *17*, 221. (e) Burchell, T. J.; Eisler, D. J.; Puddephatt, R. J. *Inorg. Chem.* **2004**, *43*, 5550.
- (10) Nam, H. J.; Lee, H. J.; Noh, D. Y. *Polyhedron* **2004**, *23*, 115.
- (11) (a) Sarker, K. K.; Chand, B. G.; Suwa, K.; Cheng, J.; Lu, T. H.; Otsuki, J.; Sinha, C. *Inorg. Chem.* **2007**, *46*, 670. (b) Dai, J.; Wang, X.; Bian, G. Q.; Zhang, J. S.; Guo, L.; Munakata, M. *J. Mol. Struct.* **2004**, *690*, 115. (c) Garoufis, A.; Perlepes, S.; Schreiber, A.; Bau, R.; Hadjiliadis, N. *Polyhedron* **1996**, *15*, 177.
- (12) (a) He, M.; Twieg, R. J.; Gubler, U.; Wright, D.; Moerner, W. E. *Chem. Mater.* **2003**, *15*, 1156. (b) Justin Thomas, K. R.; Lin, J. T.; Tao, Y. T.; Chuen, Ch. H. *Chem. Mater.* **2002**, *14*, 3852. (c) Liu, B.; Yu, L. W.; Lai, Y. H.; Huang, W. *Chem. Mater.* **2001**, *13*, 1984. (d) Ko, Ch. W.; Tao, Y. T.; Lin, J. T.; Justin Thomas, K. R. *Chem. Mater.* **2002**, *14*, 357. (e) Chun, H.; Moon, I. K.; Shin, D. H.; Kim, N. *Chem. Mater.* **2001**, *13*, 2818.
- (13) Zhou, H. P.; Wang, P.; Hu, Z. J.; Li, L.; Chen, J. J.; Cui, Y.; Tian, Y. P.; Wu, J. Y.; Yang, J. X.; Tao, X. T.; Jiang, M. H. *Eur. J. Inorg. Chem.* **2007**, 1854.
- (14) Sheldrick, G. M.; *SHELXL-97*, Program for the Refinement of Crystal Structures; University of Göttingen, Göttingen, 1997.
- (15) Parr, R. G.; Young, W. *Density Functional Theory of Atoms and Molecules*; Oxford University Press: New York, 1989.
- (16) Vosko, S. H.; Wilk, L.; Nusair, M. *Can. J. Phys.* **1980**, *58*, 1200.
- (17) (a) Versluis, L.; Ziegler, T. *J. Chem. Phys.* **1988**, *88*, 322. (b) Fan, L.; Ziegler, T. *J. Chem. Phys.* **1991**, *95*, 7401.
- (18) Perdew, J. P.; Chevary, J. A.; Vosko, S. H.; Jackson, K. A.; Pederson, M. R.; Singh, D. J.; Fiolhais, C. *Phys. Rev.* **1992**, *46*, 6671.
- (19) Lenthe, E.; Ehlers, A.; Baerends, E. J. *J. Chem. Phys.* **1999**, *110*, 8943.
- (20) William, L. J.; Daniel, L. S. *J. Am. Chem. Soc.* **1990**, *112*, 4168.
- (21) Mak, T. C. W.; Wu, Y. K. *Inorg. Chim. Acta* **1985**, *104*, 149.
- (22) (a) Grdenic, D. *Quart. Rev.* **1965**, *19*, 303. (b) Grdenic, D. *Connections in the Crystal Structures of Mercury Compounds. In Structural Studies of Molecules of Biological Interest*; Dodson, G., Glusker, J. P., Sayre, D., Eds.; Clarendon Press, Oxford, UK, 1981, 207. (c) Pauling, L. *The Nature of the Chemical Bond*, 3rd ed.; Cornell University Press: Ithaca, NY, 1960.
- (23) (a) Pauling, L. *The nature of the chemical bond*; Cornell University Press: New York, 1939. (b) Pauling, L.; Pauling, P. *Chemistry*; W. H. Freeman Company: San Francisco, CA, 1975. (c) Bondi, A. J. *Phys. Chem.* **1964**, *68*, 441. (d) Bokii, G. B. *Kistalokhimiya. In Crystal Chemistry*; Nauka: Moscow, Russia, 1971.
- (24) (a) Diefenbach, U.; Adamaszek, P.; Bloy, M.; Kretschmann, M.; Scholz, S. Z. *Anorg. Allg. Chem.* **1998**, *624*, 1679. (b) Falvello, L. R.; Fornieś, J.; Martin, A.; Navarro, R.; Sicilia, V.; Villarroya, P. *Inorg. Chem.* **1997**, *36*, 6166. (c) Laavanya, P.; Venkatasubramanian, U.; Panchanatheswaran, K.; Krause, J. A. *Chem. Commun.* **2001**, 1660. (d) Pickardt, J.; Wischinski, P. Z. *Anorg. Allg. Chem.* **1999**, *625*, 1527.
- (25) (a) Moorthy, J. N.; Natarajan, R.; Mal, P.; Venugopalan, P. *J. Am. Chem. Soc.* **2002**, *124*, 6530. (b) Burchell, T. J.; Puddephatt, R. J. *Inorg. Chem.* **2005**, *44*, 3718. (c) Matsumoto, A.; Tanaka, T.; Tsubouchi, T.; Tashiro, K.; Saragai, S.; Nakamoto, S. *J. Am. Chem. Soc.* **2002**, *124*, 8891. (d) Sharma, J. A. R. P.; Desiraju, G. R. *Acc. Chem. Res.* **1986**, *19*, 222.
- (26) (a) Metrangolo, P.; Neukirch, H.; Pilati, T.; Resnati, G. *Acc. Chem. Res.* **2005**, *38*, 386. (b) Desiraju, G. R.; Parthasarathy, R. *J. Am. Chem. Soc.* **1989**, *111*, 8725.
- (27) Sun, Sh.-Sh.; Lees, A. J. *Coord. Chem. Rev.* **2002**, *230*, 170.
- (28) Balzani, V.; Juris, A.; Venturi, M.; Campagna, S.; Serroni, S. *Chem. Rev.* **1996**, *96*, 759.
- (29) (a) Ciurtin, D. M.; Pschirer, N. G.; Smith, M. D.; Bunz, U. H. F.; zur Loye, H. C. *Chem. Mater.* **2001**, *13*, 2743. (b) Cariati, E.; Bu, X.; Ford, P. C. *Chem. Mater.* **2000**, *12*, 3385. (c) Würthner, F.; Sautter, A. *Chem. Commun.* **2000**, 445.